Original papers
Manufacturing processes and systems

УДК 546.26-162 DOI: 10.17277/jamt-2026-11-01-043-056

Investigation of the crystal structure, morphological and dispersion properties of carbon components of colloidal solutions based on natural graphite and carbon black

© Natalia N. Goncharova[a]✉, Vladimir M. Samoilov[b], Egor A. Danilov[b], Anastasiya V. Nakhodnova[b], Boris S. Kleusov[b], Maksim V. Gudkov[c], Nikolai I. Novosadov[c], Vlada A. Goncharova[b]

[a] *Private institution for the scientific development of the nuclear industry* "*Science and innovation*", *Bld. 4, 44, Bolshaya Ordynka, Moscow, 119017, Russian Federation;*
[b] *JSC Scientific Research Institute of Structural Materials Based on Graphite* "*NIIgrafit*", *2, Elektrodnaya St., Moscow, 111524, Russian Federation;*
[c] *N. N. Semenov Federal Research Center for Chemical Physics Russian Academy of Sciences, Bld. 1, 4, Kosygina St., Moscow, 119991, Russian Federation*

✉ ng6190089@gmail.com

Abstract. Results of a comparative study of the crystal structure of carbon components in nanodispersed liquid colloidal solutions based on natural graphite (NG) and carbon black, obtained by grinding combined with chemical cleavage (oxidation with a mixture of nitric and sulfuric acids), are presented. For the studied samples, structural features, average particle size, electrical conductivity and diffuse reflectance coefficient were determined. The studies revealed fundamental differences in both the structure of the carbon components of the colloidal solutions based on NG and carbon black, and the properties of coatings produced from them. In the case of NG, this is nanodispersed graphite, which retains the structure of the original NG even after grinding and chemical cleavage. Despite the destruction of the original crystallites along the basal planes, few-layer graphene particles were not found, and the resulting particles are NG nanocrystallites with a three-dimensionally ordered crystalline structure. The carbon component of the carbon black-based colloidal solution is also a nanodispersed polycrystalline graphite-like material, but has a turbostratic structure inherent to the original carbon black. These structural differences lead to fundamental disparities in coating properties from NG- and carbon black-based colloidal solutions, with surface electrical resistance of 5.10 and 55,600 kOhm·sq.$^{-1}$, respectively. For NG, coating reflectivity at a 60° light beam incidence angle was 3.0–5.0%. However, in the case of carbon black, reflectivity at 60° was 0.2–0.3%, which is anomalously low for carbon materials.

Keywords: colloidal solutions; natural graphite; carbon black; crystal structure; X-ray structural analysis; Raman spectroscopy; dynamic light scattering; electrical conductivity; reflection coefficient.

For citation: Goncharova NN, Samoilov VM, Danilov EA, Nakhodnova AV, Kleusov BS, Gudkov MV, Novosadov NI, Goncharova VA. Investigation of the crystal structure, morphological and dispersion properties of carbon components of colloidal solutions based on natural graphite and carbon black. *Journal of Advanced Materials and Technologies*. 2026;11(1):043-056. DOI: 10.17277/jamt-2026-11-01-043-056

Исследование кристаллической структуры, морфологических и дисперсионных свойств углеродных составляющих коллоидных препаратов на основе природного графита и сажи

© Н. Н. Гончарова[a]✉, В. М. Самойлов[b], Е. А. Данилов[b], А. В. Находнова[b], Б. С Клеусов[b], М. В Гудков[c], Н. И. Новосадов[c], В. А Гончарова[b]

[a] *Частное учреждение* «*Наука и инновации*», *Большая Ордынка, 44, стр. 4, Москва, 119017, Российская Федерация;*

[b] *АО «Научно-исследовательский институт конструкционных материалов на основе графита «НИИграфит», ул. Электродная, 2, Москва, 111524, Российская Федерация;*
[c] *Федеральный исследовательский центр химической физики им. Н. Н. Семенова РАН, ул. Косыгина, 4, Москва, 119991, Российская Федерация*

✉ ng6190089@gmail.com

Аннотация. Представлены результаты сопоставительного исследования кристаллической структуры углеродных составляющих нанодисперсных жидких коллоидных препаратов на основе естественного природного графита (ЕГ) и сажи, полученных методом измельчения в сочетании с химическим расщеплением (окисление смесью азотной и серной кислот). Для исследуемых образцов определяли особенности структурного строения, средний размер частиц, электропроводность и коэффициент диффузного отражения. В результате исследований установлено существование принципиальных различий как по структуре углеродных составляющих коллоидных растворов на основе ЕГ и сажи, так и по свойствам изготовленных из них покрытий. В случае ЕГ – это нанодисперсный графит, даже после измельчения и химического расщепления, сохраняющий структуру исходного ЕГ. Несмотря на разрушение исходных кристаллитов по базисным плоскостям, образования малослойных, графеновых частиц не происходит, и образовавшиеся частицы представляют собой нанокристаллиты ЕГ и имеют трехмерно упорядоченную структуру. Углеродная составляющая сажевого коллоидного раствора также является нанодисперсным поликристаллическим графитоподобным материалом, однако имеет турбостратную структуру, присущую исходной саже. Структурные различия приводят к принципиальной разнице в свойствах покрытий, полученных из коллоидных растворов на основе ЕГ и сажи по поверхностному электросопротивлению (5,10 и 55600 кОм/кв. соответственно). Для ЕГ отражательная способность покрытий при угле наклона светового луча 60° составляла (3,0 – 5,0 %). Однако для сажи отражательная способность покрытий при угле наклона светового луча 60° составляла 0,2 – 0,3 %, что является аномально низким для углеродных материалов.

Ключевые слова: коллоидные растворы; естественный графит; сажа; кристаллическая структура; рентгеноструктурный анализ; рамановская спектроскопия; динамическое светорассеяние; электропроводность; коэффициент отражения.

Для цитирования: Goncharova NN, Samoilov VM, Danilov EA, Nakhodnova AV, Kleusov BS, Gudkov MV, Novosadov NI, Goncharova VA. Investigation of the crystal structure, morphological and dispersion properties of carbon components of colloidal solutions based on natural graphite and carbon black. *Journal of Advanced Materials and Technologies*. 2026;11(1):043-056. DOI: 10.17277/jamt-2026-11-01-043-056

1. Introduction

Most domestic technologies for producing colloidal graphite and colloidal carbon black solutions using chemical cleavage were developed quite some time ago [1, 2]. Currently, nanodispersed carbon-containing colloidal solutions are highly promising for use in various fields of science and technology, including chemical, mechanical engineering, metallurgy, and other industries [2–8], rubber production [7, 8], as well as medicine [9, 10] and electronics [11, 12]. Carbon-based colloidal preparations exhibit good lubricating properties and low friction coefficient, retaining these properties at elevated temperatures, allowing their use as modifying agents [1–8], including in nanocomposites [4, 5]. Their advantage is the ability to form chemically inert films and coatings with high adhesion to the substrate upon drying. Such coatings typically possess stable electrical conductivity, along with a range of other interesting electronic and optical properties [1–5, 11, 12].

Over the years, fundamental changes have occurred in the raw material base of the carbon industry, necessitating adaptation of technological processes to new sources. Due to the expansion of application areas for colloidal preparations, requirements have changed both for carbon components and the properties of the solutions themselves. However, the most radical changes have occurred in modern research and control methods for nanodispersed systems, most of which were not used in developing traditional colloidal preparation technologies. More recent publications often focus on colloidal systems based on other starting materials (oxidized graphite, nanotubes, etc.), including those obtained in organic media or ionic liquids [13–17].

The aim of this work is a comparative study of the crystalline structure of carbon components in alcohol-based colloidal solutions based on natural graphite (NG) and carbon black, as well as properties of colloidal preparations based on them, to restore lost technology for materials used in special equipment according to old specifications.

2. Materials and Methods

2.1. Starting materials and sample preparation method

Natural graphite grade "GSM-2" (JSC "Graphite Service", Chelyabinsk) was used to prepare colloidal solutions based on NG. A weighed portion of graphite was ground in a IVCh-3 vibrational grinder for 60 min, with predominantly abrasive-crushing loads during grinding. The ground graphite was sieved through a vibrating sieve with a 63 μm mesh size to break up agglomerates and homogenize it. The resulting powder was treated with a mixture of nitric and sulfuric acids for 2–3 hours at room temperature and 45 min at 150 °C. The suspension, cooled to room temperature, was then repeatedly rinsed with distilled water until pH reached approximately 6–7 (washing by decantation). The resulting solution was dried to constant weight at 120 °C in an ES-4610 drying oven (Ekos, Russia) equipped with forced circulation. The dry residue was dispersed in ethanol using an ultrasonic bath SONOREX SUPER RK 100H (Bandelin, Germany).

Colloidal solutions based on "T-900" carbon black grade were prepared in a similar manner.

2.2. Methods for determining sample properties

The concentration of the carbon component in colloidal solutions was determined by the mass of dry residue, via evaporation of the liquid dispersion medium at 120 °C in an ES-4610 drying oven.

Dynamic viscosity of colloidal carbon black and colloidal graphite solutions was measured using a spindle rotational viscometer FUNGILAB EVO EXPERT. Prior to measurements, a 50 mL sample underwent additional dispersion in an ultrasonic laboratory disperser MEF 98 (LLC "Melfiz", Moscow) at a working frequency of 28 kHz and ultrasound intensity of 250 $W \cdot cm^{-2}$ for 5 min to prevent thixotropy typical of such solutions.

Particle size distributions were determined using a Malvern Instrument Zen 1600 by dynamic light scattering. For analysis, 2 mg of suspension (concentration 55 $mg \cdot L^{-1}$) was mixed with 500 mL distilled water, followed by final ultrasonic disperser МЭF 98 treatment for 2 min.

Optical density of graphite colloidal solutions was determined using a "SF-2000" spectrophotometer in the wavelength range 190–1100 nm [9, 10]. Samples of colloidal graphite and colloidal carbon black solutions at 55 $mg \cdot L^{-1}$ concentration underwent final ultrasonic disperser MEF 98 treatment for 5 min.

Specific surface area of the original graphite and carbon black powders was determined by physical nitrogen adsorption on solid surfaces and BET method calculation per Russian Standard 13144-79. Specific surface area of graphite particles in suspension was determined by methylene blue adsorption method, involving titration of graphite suspension with 0.3 % methylene blue solution in the presence of sulfuric acid presence. Specific surface area was calculated based on methylene blue consumed for sample titration.

Dry residue samples from NG and carbon black suspensions were studied by Raman spectroscopy using a confocal Raman microspectrometer in Via Reflex (Renishaw, UK) at 532 nm wavelength (solid-state Nd:YAG laser with diode pumping). Laser power did not exceed 1 mW, with a laser spot diameter of ~5 μm. Signal acquisition time was 5 s, with 30 spectra recorded per sample. Prior to analysis, a sample (at least 0.1 mL) was placed liquid on a monocrystalline silicon substrate plate and dried with hot air. Data determined positions of main *D*, *G*, and 2*D* lines, and intensity ratios I_D/I_G and I_{2D}/I_G [18–22].

X-ray structural analysis was performed on a D8 Advance powder diffractometer (Bruker, Germany) using copper K_α radiation ($\lambda = 0.15418$ nm) in θ–2θ scanning mode. Scan step was 0.02°, speed $10° \cdot min^{-1}$ for graphites and $2° \cdot min^{-1}$ for carbon black. Samples were applied to polycrystalline silicon substrates prior to analysis. Diffraction data determined interplanar spacing d_{002}, L_c parameter (coherent scattering region perpendicular to layer), and graphitization degree *g* [23, 24].

The degree of graphitization is calculated using formula (1):

$$g = \frac{(0.344 - d_{002})}{(0.344 - 0{,}335)}, \quad (1)$$

where 0.344 nm is the interlayer distance of a substance with a completely disordered structure; 0.335 nm is the interlayer distance of a graphite monocrystal; and d_{002} is the interlayer distance of the studied material, nm.

Surface electrical resistance of coatings with thickness of at least 6 μm was determined by the four-electrode method using a specially assembled setup compliant with the main methods for controlling surface and specific resistance of films based on carbon nanotubes (CNT) per Russian Standard IEC/TS 62607-2-1-2017 [25]. Measurements were performed on pairwise independent terminals of the source-meter.

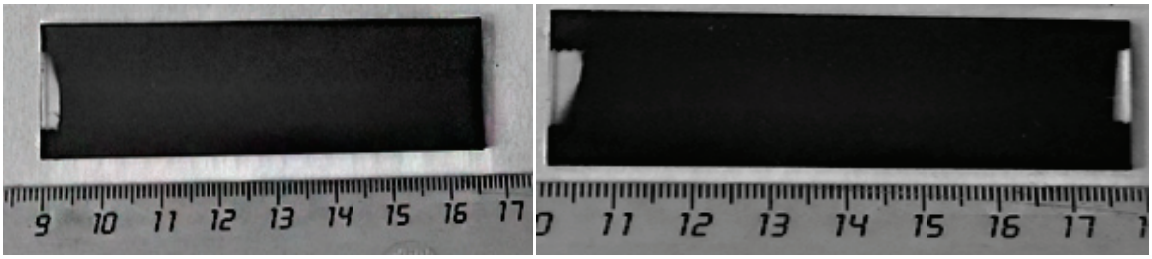

(a) *(b)*

Fig. 1. Appearance of coatings based on colloidal solutions of NG (*a*) and carbon black (*b*) on a glass substrate

For specific resistivity evaluation, film thickness was measured using an Absolute C112XBS micrometer (Mitutoyo, Japan) with 1 μm accuracy. The film sample was applied to glass and pressed in a cell with a counterpiece (also made of polished polymethyl methacrylate). Current supply to outer electrodes (I_{14}) and voltage difference measurement between inner electrodes (V_{23}) were performed using a precision source-meter B2901a (Keysight, USA) with compensation for source current/voltage leakage resistance. Full volt-ampere characteristics of samples were measured, and V_{23}/I_{14} values were determined in the linearity range. To minimize thermo-emf error, measurements were conducted pairwise with current direction reversal and result averaging [26].

Surface electrical resistance of the coating was calculated using formula (2):

$$\rho = 2\pi s \frac{V_{23}}{I_{14}} F_i , \qquad (2)$$

where ρ is surface electrical resistance, Ω·m; s is sample thickness, m; $F_i = 0.706$ is a correction factor depending on sample size, inter-probe distance, conductive film thickness, and probe-to-edge distance [26].

Diffuse reflectance/transmittance coefficients of coating samples were determined spectrophotometrically using a Cary-5000 UV-VIS-NIR spectrophotometer with UMA accessory (Agilent, USA). Pre-treated ultrasonic disperser colloidal solutions based on NG and carbon black were airbrushed onto cleaned microscope slide surfaces to form continuous uniform opaque coatings on one side.

General view of samples for Raman spectra recording, as well as for surface electrical conductivity and diffuse reflectance coefficients R measurements based on NG and carbon black, is shown in Fig. 1.

Sample measurements were performed at the center using "Full" light beam without diaphragm, with 1 nm wavelength step, and "Auto/3" energy level. Diffuse reflectance coefficients R were measured at incidence angles on coating surface of 6°, 15°, 30°, 45°, 60° (full angles relative to light source and detector axes were 12°, 30°, 60°, 90°, and 120°, respectively). Note that 25–650 and 650–2500 nm ranges use different light sources, with data recorded by detectors of varying sensitivity, causing observed "jump" at 650 nm and below. The data obtained in this range reflect only qualitative reflectance changes.

3. Results and Discussion

Raman spectra of initial, ground, and ground-then-oxidized "GSM-2" graphite and "T-900" carbon black samples are shown in Figs. 2 and 3. Numerical values of selected parameters from Raman spectra (Figs. 2 and 3) are given in Table 1.

The main parameters of the Raman spectra of NG and carbon black: the position of the main peaks G, D and $2D$ (ω_D, ω_G и ω_{2D}), as well as the ratios of their integrated intensities (I_D/I_G, I_G/I_{2D}), are given in Table 1.

The Raman spectra of NG samples shown in Fig. 2 before and after grinding are typical for graphite-like materials [18–22]. The I_{2D}/I_G ratio remains low (~0.5, see Table 1), even after chemical cleavage, which is uncharacteristic of few-layer graphene particles that exhibit $I_{2D}/I_G \sim 1$ [19, 22]. In the spectrum of initial NG, the D peak has low intensity, indicating low defectiveness of the crystal structure. After intensive grinding and subsequent chemical cleavage, the D peak intensity increases (see Fig. 2*b*, *c*), signaling increased crystalline structure defectiveness relative to initial NG, consistent with literature data [18–22].

In the Raman spectrum of NG after chemical cleavage, a supplementary peak appears at ~1620 cm^{-1} near the G band (1575 cm^{-1}). This peak, typically called D' in literature [25–27], has unclear origin. It is absent in highly oriented pyrolytic carbon and glassy carbon samples [18, 28], but present in nanocrystalline graphite subjected to neutron

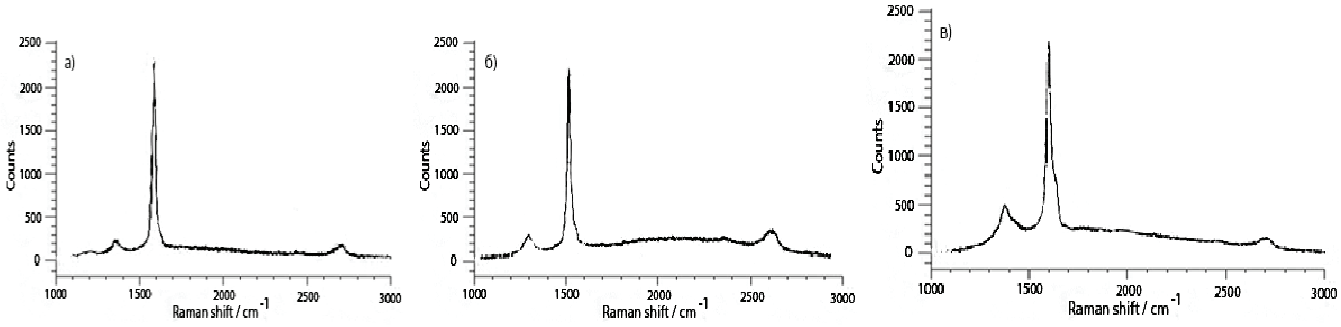

(a) *(b)* *(c)*

Fig. 2. Raman spectra of GSM-2 graphite samples: (*a*) initial material; (*b*) after grinding; (*c*) after chemical cleavage

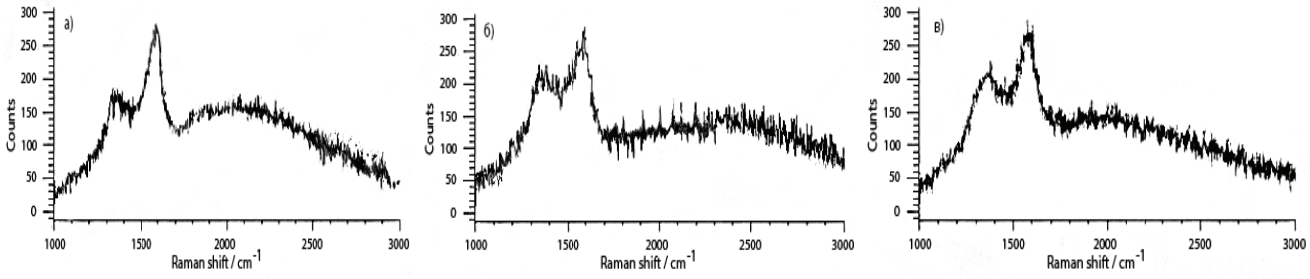

(a) *(b)* *(c)*

Fig. 3. Raman spectra of T-900 carbon black samples: (*a*) initial material; (*b*) after grinding; (*c*) after chemical cleavage

Table 1. Main parameters of the Raman spectra of NG and carbon black

Sample	Position of peak *D*, cm^{-1}	Position of peak *G*, cm^{-1}	Position of peak 2*D*, cm^{-1}	I_D/I_G, rel. units	I_{2D}/I_G, rel. units
Graphite GSM-2, initial	1352	1579	2705	0.163	0.626
Graphite GSM-2, ground	1352	1575	2695	0.495	0.378
Graphite GSM-2, ground, after chemical cleavage	1351	1576	2691	0.528	0.412
Carbon black T900, initial	1366	1589	–	2.265	–
Carbon black T900, ground	1364	1590	–	2.135	–
Carbon black T900, ground, after chemical cleavage	1362	1590	–	2.070	–

irradiation, where its intensity grows with irradiation dose and crystallite size reduction due to defect increase [25–27]. In chemically cleaved graphites, such defects primarily include in-plane defects like monovacancies, divacancies, and Stone-Thrower-Wales defects, etc. [27, 29].

Raman spectra of initial carbon black are also typical for carbon materials with turbostratic structure and low crystal perfection [30–32]. The 2D peak is absent, characteristic of materials with low graphitization degree [30]. Observed spectra match carbon black produced at 1000–1500 °C [30–32]. Grinding and chemical cleavage cause minimal changes to initial carbon black crystal structure (see Fig. 3*b*, *c*).

Diffraction patterns of initial, ground, and ground-then-chemically-cleaved "GSM-2" graphite and "T-900" carbon black are shown in Figs. 4 and 5, respectively; numerical values of obtained crystal structure parameters are given in Table 2.

In the diffraction patterns of initial NG, two intense lines corresponding to (002) and (004) reflections are observed. The (004) line represents the K_α doublet of the characteristic X-ray tube spectrum.

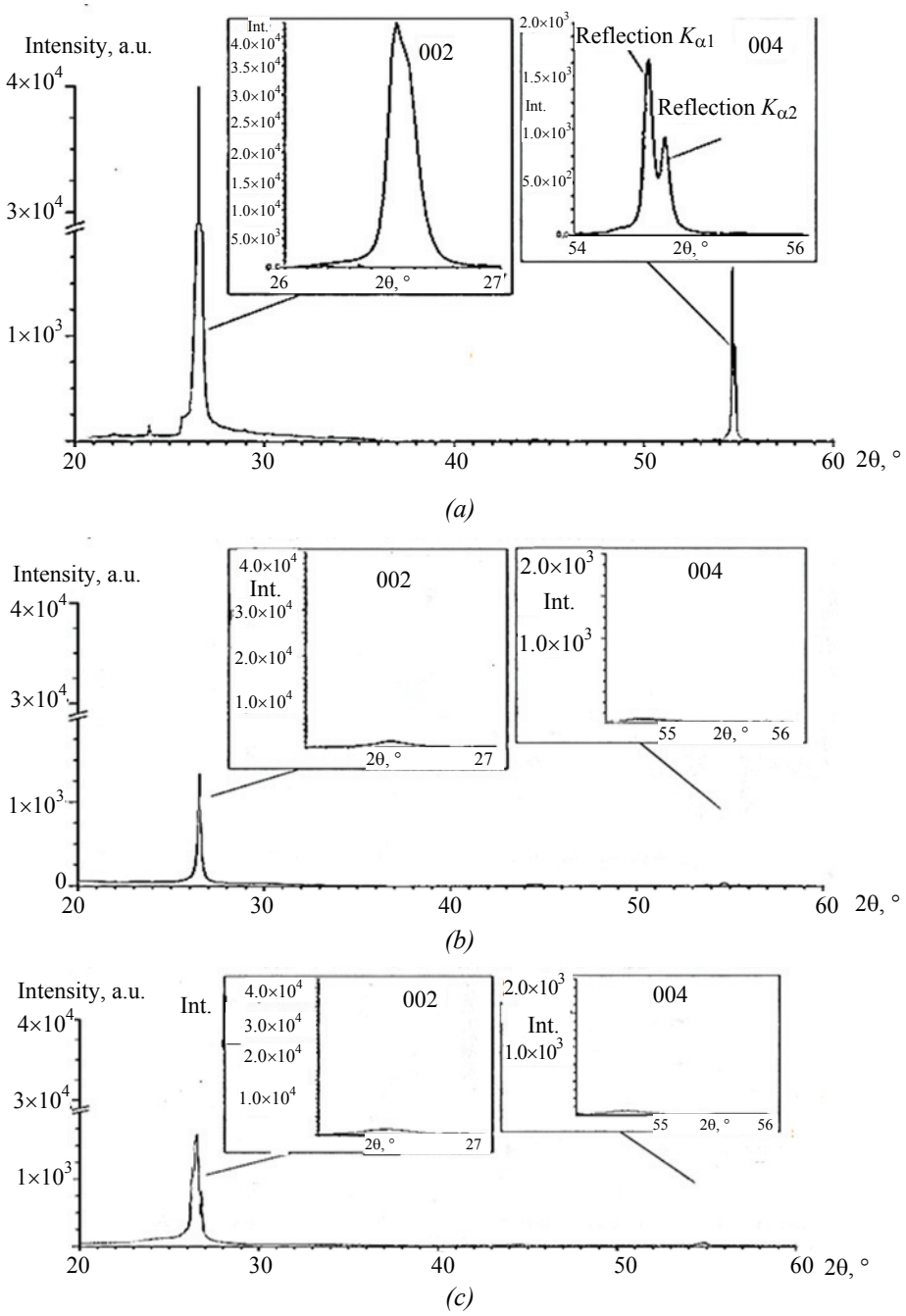

Fig. 4. Diffractograms of GSM-2 graphite samples: (*a*) initial material; (*b*) after grinding; (*c*) after chemical cleavage

In diffraction patterns of ground and ground-then-oxidized graphite, diffraction lines shift toward lower angles, primarily due to significant reduction in sample texturing after grinding. The intensity of the (002) diffraction line sharply decreases after grinding and chemical cleavage, as particle size reduction of initial NG, accompanied by decreased crystal structure perfection, weakens diffracted radiation intensity and broadens diffraction maxima [33, 34]. However, the interlayer spacing remains virtually unchanged (see Table 2), confirming that the material remains graphitic in structure.

In carbon black diffraction patterns, two lines are observed: (002) and (011). Broad lines correspond to high structural defectiveness of carbon black. X-ray structural analysis data were used to calculate interplanar spacing d_{002}, L_c size (along (002) direction), and graphitization degree. Results are presented in Table 2.

According to Table 2 data, intensive NG cleavage occurs already in ground samples, apparently due to predominant abrasive-crushing loads, and continues during chemical cleavage. However, d_{002} increase typical for high-load milling [33, 34] does not occur.

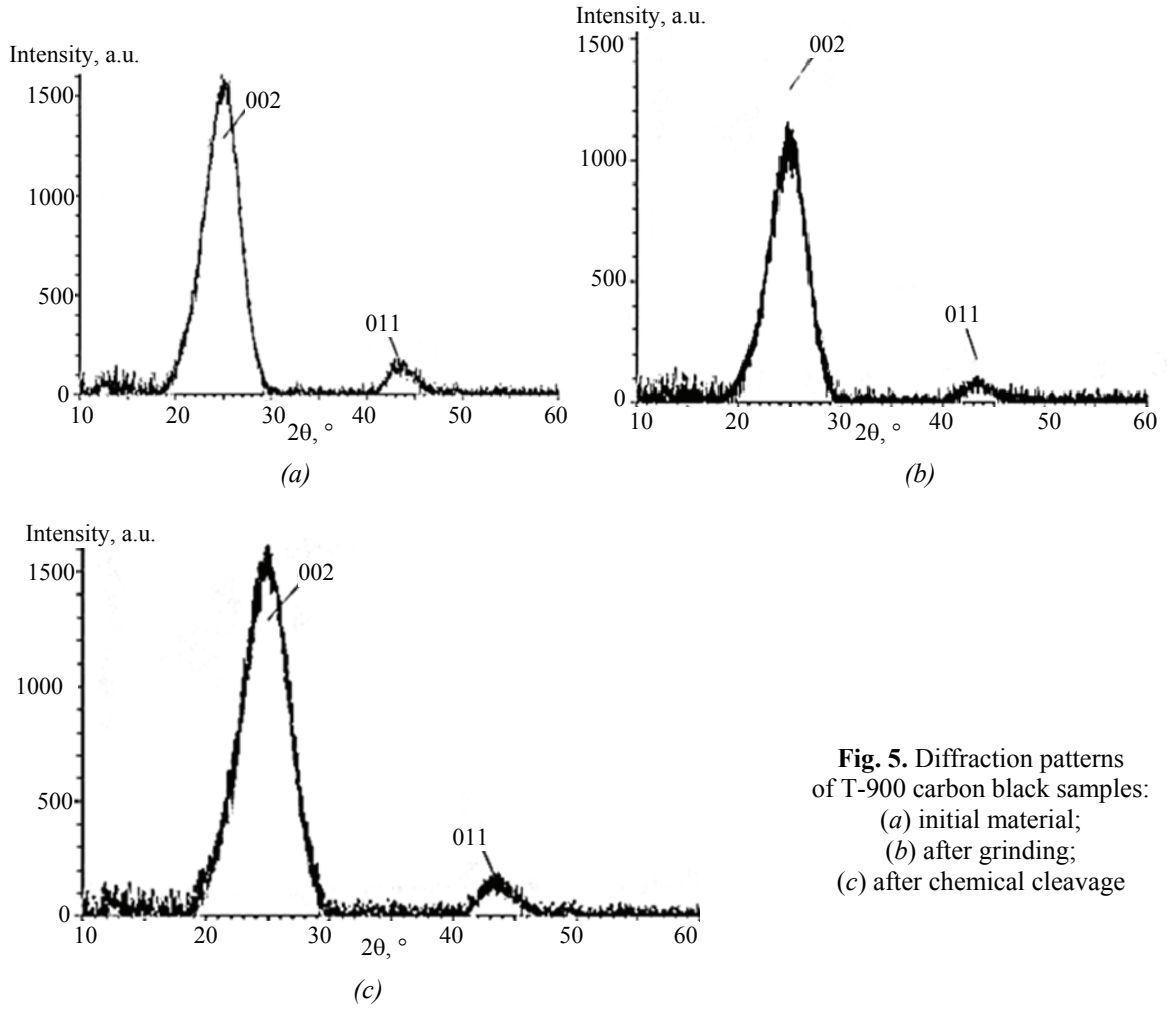

Fig. 5. Diffraction patterns of T-900 carbon black samples: (*a*) initial material; (*b*) after grinding; (*c*) after chemical cleavage

Table 2. Results of X-ray diffraction analysis of NG and carbon black

Sample	d_{002}, nm	*g*, %	L_c, nm	*N**
Graphite GSM-2 initial	0.3355	99	164	460
Graphite GSM-2 ground	0.3358	96	45	130
Graphite GSM-2 ground, after chemical cleavage	0.3358	96	26	70
Carbon black T900 initial	0.3683	0	1.3	4
Carbon black T900 ground	0.3688	0	1.3	4
Carbon black T900 ground, after chemical cleavage	0.3690	0	1.4	4

Thus, based on L_c values (see Table 2), initial NG crystallites contain ~460 graphene layers (*N**), reducing to ~130 layers after grinding and ~70 layers after chemical cleavage. Note that the latter estimate applies to larger graphite particles least affected by chemical cleavage, as complete NG cleavage eliminates the (002) line [34, 35]. It should also be noted that signs of the formation of graphite oxide after chemical cleavage in the form of an intense peak at 2θ of the order of 13–15° [36] are absent in the diffraction patterns (see Fig. 4*b*, *c*).

For carbon black samples, intensive grinding and chemical cleavage cause virtually no substantial changes in crystal structure parameters (see Table 2), apparently due to low sensitivity of X-ray phase analysis for ~1 nm crystallite sizes [27, 31]. Graphite oxide formation signs after chemical cleavage (intense peak at 2θ ~ 13–15°) [36] are also absent in carbon black diffractograms (see Fig. 5*b*, *c*).

Particle size measurement results for NG- and carbon black-based colloidal solutions by dynamic light scattering are shown in Fig. 6. Maximum particle size

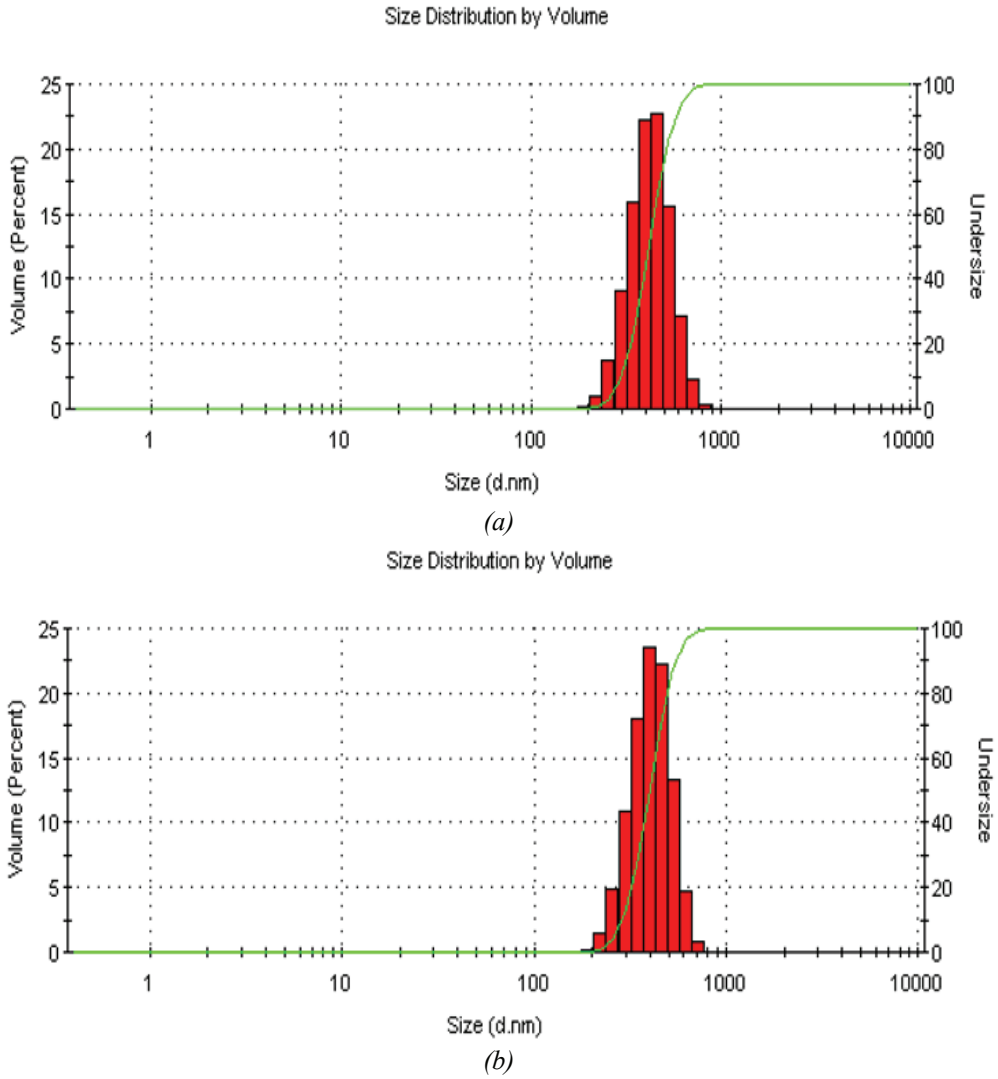

Fig. 6. Particle size distribution in colloidal solutions based on GSM-2 NG (*a*) and T-900 carbon black (*b*)

for both colloidal graphite and colloidal carbon black solutions does not exceed 1000 nm, with similar average sizes of 281 and 301 nm, respectively.

Raman spectra and SEM data of the surface of dry residues of dried colloidal solutions based on NG and carbon black are presented in Fig. 7. As can be seen, the ratio of the integrated intensities of the *D* and *G* lines (I_D/I_G) on the coating samples differ little from each other and remain approximately the same as on the samples dried after chemical cleavage (see Table 1).

The results of measuring the diffuse reflectance spectra of coatings based on colloidal solutions of NG and carbon black are presented in Fig. 8.

As the angle of light beam incidence decreases, the reflectivity of NG-based coatings decreases. At maximum light beam incidence angle (60°), reflectivity in the 650–2000 nm range increases from 3 to 5 %. Considering graphite is a well-studied material often used as an "absolute black body" in pyrometric high-temperature measurements, reference values of total emissivity at 300 K [23, 37] confirm the obtained reflectance coefficients for NG-based coatings.

However, for carbon black-based coatings, the reflectance coefficient drops sharply and the dependence pattern changes: in the 650–2000 nm range, carbon black coating reflectivity increases but remains within very low values. At maximum light beam incidence angle (60°), carbon black coating reflectivity ranges from 0.18 to 0.32 %. These values are nearly an order of magnitude lower than known total emissivity values for other carbon materials [23, 37], with minimum reflectance coefficients observed in highly oriented pyrolytic graphite samples when infrared radiation is directed at edge faces [23, 37].

In recent years, anomalously low reflectance values (0.1–0.01 %) have been found in coatings consisting of vertically oriented carbon nanotubes [38–40], explained by the simultaneous combination of high proportion of prismatic faces with deep

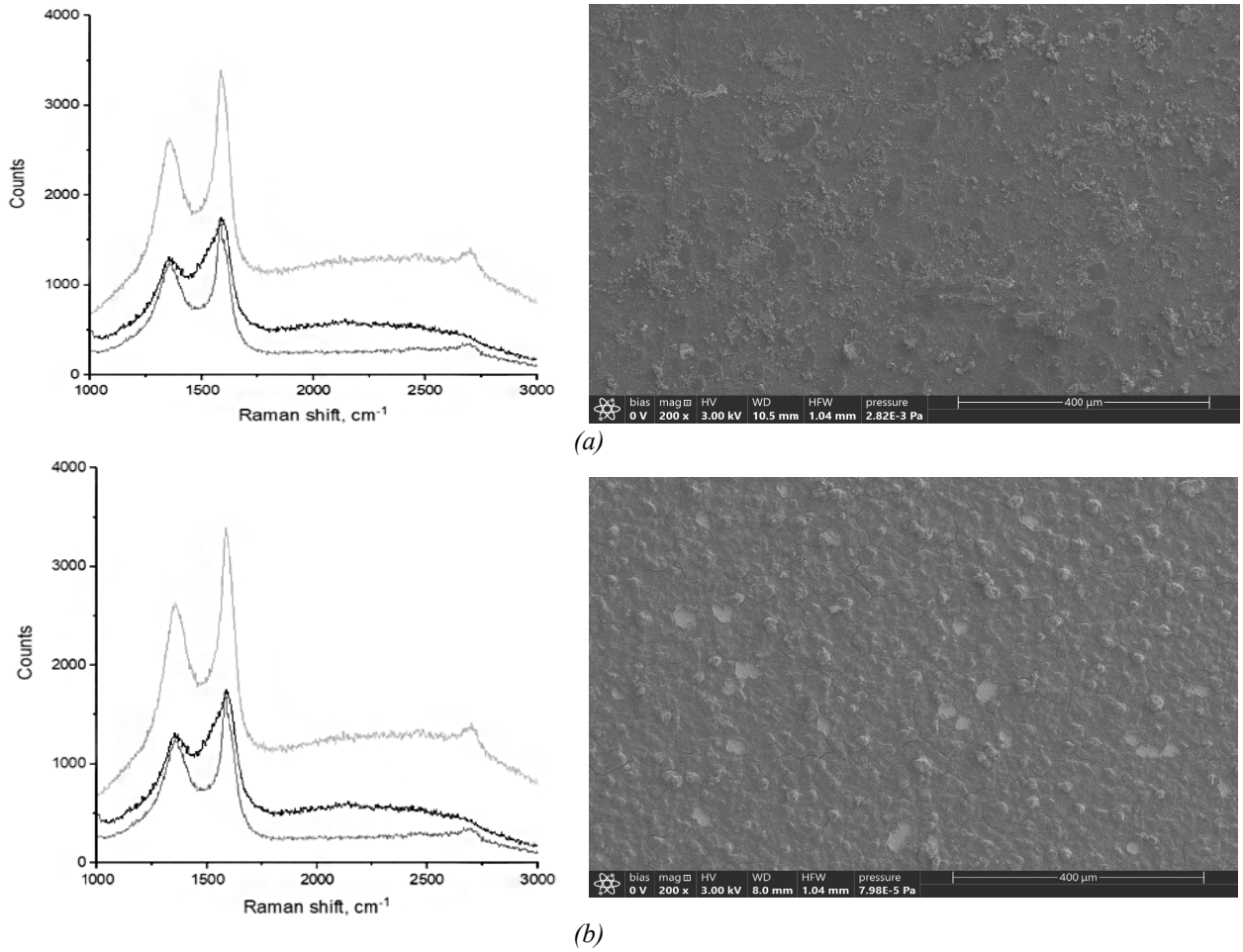

Fig. 7. Raman spectra and SEM images of the surface of coatings: (*a*) NG-based; (*b*) carbon black-based

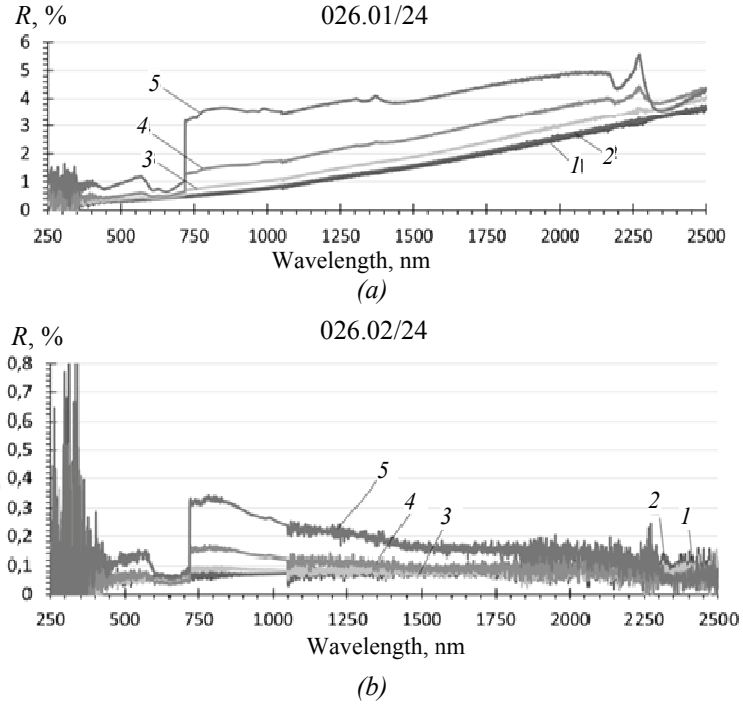

Fig. 8. Results of measurements of spectral dependencies of the reflection coefficients *R* at various angles for coating samples deposited from colloidal solutions: (*a*) NG-based; (*b*) carbon black-based (*1* – *R* = 6°; *2* – *R* = 15°; *3* – *R* = 30°; *4* – *R* = 45°; *5* – *R* = 60°)

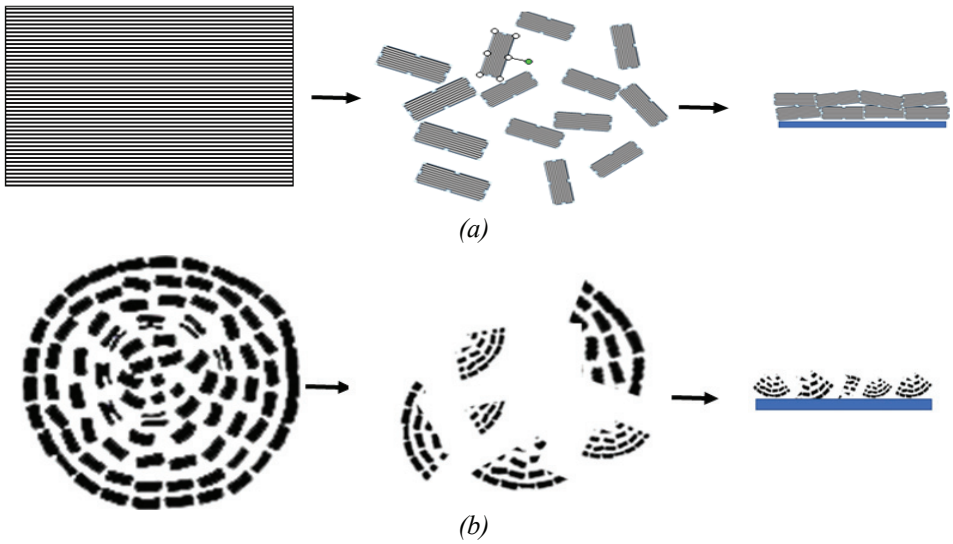

(a)

(b)

Fig. 9. Scheme of NG (*a*) and carbon black (*b*) particle transformation during thermochemical decomposition

nanopores formed by outer walls of adjacent nanotubes. Such high absorption capacity of colloidal carbon black-based coatings is difficult to explain. Presumably, NG and carbon black particle destruction during chemical cleavage occurs completely differently, as shown in Fig. 9.

NG cleavage predominantly occurs along basal planes, and NG-based coating particles' basal planes are primarily oriented parallel to the substrate surface, resulting in typical reflectivity for graphite-like carbon materials [23, 37].

In contrast, due to peculiarities of their crystalline structure, carbon black particles during chemical cleavage break into irregularly shaped segments [41, 42]. Accordingly, carbon black-based coatings consist of chaotically oriented and very small crystallites. A significant portion of carbon black-based coating surface will be formed not only by poorly oriented basal planes but also prismatic faces of crystallites. In addition, carbon black is characterized by a significant volume of nanoporosity in a wide range of sizes [43, 44], the accessibility of which increases as a result of chemical decomposition and destruction of spherical carbon black particles, which are preserved in the coating. The combination of nanoporosity-induced channels and high proportion of prismatic faces apparently causes near-complete light beam absorption by carbon black-based coatings.

The data on the electrical conductivity of the coatings seems to be interesting. Conductivity of few-layer graphene-based coatings can reach 150–200 $\Omega \cdot sq.^{-1}$ [45, 46], though these data pertain to coatings from particles not subjected to acid treatment and intensive grinding. In our case, NG-based coating surface electrical resistance measured (5.10 ± 0.05) $k\Omega \cdot sq.^{-1}$, is comparable to graphite colloidal preparation "C-1" film produced per TU 113-08-48-63-90 $((3.81 \pm 0.04)$ $k\Omega \cdot sq.^{-1})$. NG-based film surface electrical resistance proved substantially lower than carbon black-based films $((55.600 \pm 3.338)$ $k\Omega \cdot sq.^{-1})$, can be explained by larger NG crystallite sizes and correspondingly reduced role of contact resistances in charge transfer within the film.

Notably, despite elevated surface electrical resistance values of films from preparations obtained in this work compared to literature data on pure initial carbon materials [45, 46], our coatings exhibited noticeable conductivity uncharacteristic of carbon materials oxidized under more aggressive conditions. This fact, combined with absence of structural property changes in dispersed particles related to basal plane atom oxidation (interlayer spacing increase), suggests that under selected acid treatment conditions, oxidation and functionalization primarily affect edge atoms and prismatic faces. This yields sedimentation-resistant preparations whose carbon particles retain main properties of initial carbon materials, though peripheral functional groups on colloidal particles increase contact resistances. Accordingly, film conductivity differences are explained by crystallite size variations and intrinsic conductivity of initial carbon materials [47, 48].

Optical properties (reflectance at 60° light beam angle: 3.0–5.0 % and 0.2–0.3 %), NG- and carbon black-based films differ sharply, confirming the earlier conclusion about critical influence of initial carbon material structure on acid-treated preparation characteristics.

Main characteristics of obtained colloidal graphite and colloidal carbon black solutions are presented in Table 3.

Table 3. Main characteristics of the obtained colloidal graphite and colloidal carbon black solutions

Characteristic	Colloidal graphite solution	Colloidal carbon black solution	Standard colloidal graphite solutions TU 113-08-48-63-90 [51]
Dispersion medium	Ethanol	Ethanol	Water
Particle concentration (dry residue), $g \cdot L^{-1}$	55	55	Not specified
Ash content, % max	0.3	0.3	1.0–2.0
Average particle size, nm	281.87	310.86	1000–30000
Dynamic viscosity, mPa·s	3.23	1.32	–
Specific surface area of carbon component, $m^2 \cdot g^{-1}$	1839	1944	10–80*
Reduction of carbon component concentration after 1-hour settling, % max	< 1.0	< 1.0	40**
Optical density, rel. units	0.651	0.762	–
Surface electrical resistance of 200 μm thick coating, $k\Omega \cdot sq.^{-1}$	5.10 ± 0.05	55600 ± 3338	3.81 ± 0.04
Coating reflectance (60°, 750 nm), %	3.2	0.32	5.3

* experimental data;
** at 15 % mass concentration.

Unfortunately, modern domestic carbon-based colloidal preparation standardization is clearly insufficient: Russian Standard 5261 for known colloidal graphite grades (C-0, C-1, C-2, C-3) has lapsed; current specifications (e.g., TU 113-08-48-63-90 JSC "Graphite Service", Chelyabinsk) regulate very limited parameters, i.e. particle size, ash content, moisture, etc. Nanodispersed colloidal solutions obtained in this work contain submicron NG and carbon black particles, exhibit low dynamic viscosity, and sufficient stability. Note that during prolonged storage (> 10–20 days), concentration reduction may reach several percent, but re-dispersion via ultrasonication easily restores original preparation characteristics.

4. Conclusion

Colloidal solutions based on NG and carbon black contain carbon components fundamentally differing in crystalline structure. For NG, these are nanodispersed graphite particles retaining initial NG structure even after grinding and chemical cleavage. Despite destruction of original crystallites along basal planes, few-layer graphene particles do not form; resulting particles are NG nanocrystallites with three-dimensionally ordered structure. NG nanocrystallite surfaces are substantially functionalized, indicated by high stability of obtained aqueous colloidal solutions despite low conductivity of resulting coatings.

The carbon black colloidal solution carbon component is also nanodispersed polycrystalline graphite-like material but has turbostratic structure inherent to initial carbon black. Grinding and chemical cleavage cause virtually no changes in carbon black crystalline structure parameters. However, due to small crystallite sizes and disordered crystal structure, carbon black particle surfaces undergo substantially greater functionalization than NG, causing conductivity drop in carbon black-based coatings compared to NG-based ones. Low reflectance of carbon black coatings is presumably linked to primary carbon black particle destruction during grinding and chemical cleavage. This combination of factors results in fundamental differences in coating properties from NG- and carbon black-based colloidal solutions: surface electrical resistance (5.10 and 55.600 $k\Omega \cdot sq.^{-1}$, respectively) and reflectance at 60° light beam angle (3.0–5.0 % and 0.2–0.3 %, respectively).

Preliminary grinding combined with chemical cleavage enables production of nanodispersed colloidal solutions based on NG and carbon black meeting modern requirements for average particle size (< 500 nm), dry residue content (55 $g \cdot L^{-1}$), and suspension dynamic viscosity (1.3–3.2 Pa·s). These factors contribute to good dispersibility of obtained solutions with sufficiently high stability exceeding that of solutions containing larger particles.

Obtained solutions can be used as starting components for carbon coatings and sensors with special electronic/optical properties. Similar colloidal preparations may serve as effective nanocomposite modifiers, though this requires additional research beyond this work's scope.

5. Funding

The present study did not receive any external funding.

Финансирование

Настоящее исследование не получило внешнего финансирования.

6. Conflict of interests

The authors declare no conflict of interest.

Конфликт интересов

Авторы заявляют об отсутствии конфликта интересов.

References

1. Fialkov AS. *Interlayer compounds and composites based on it*. Moscow: Aspekt-press; 1998. 717 p. (In Russ.)

2. Rashed MN, editor. *Colloids: types, preparation and applications*. IntechOpen; 2021. 232 p. DOI:10.5772/intechopen.92521

3. Chen K, Xue D. Preparation of colloidal graphene in quantity by electrochemical exfoliation. *Journal of Colloid and Interface Science*. 2014;436:41-46. DOI: 10.1016/j.jcis.2014.08.057

4. Park SK, Park BJ, Cho WB, Shin EJ, et al. A semipermanently stable, photocrosslinkable graphene colloid: a fresh strategy for fabricating polymer nanocomposites. *Composites Part A: Applied Science and Manufacturing*. 2025;190:108693. DOI:10.1016/j.compositesa.2024.108693

5. Bhattacharya S, Dhar P, Das SK, Ganguly R, et al. Colloidal graphite/graphene nanostructures using collagen showing enhanced thermal conductivity. *International Journal of Nanomedicine*. 2014;9(1):1287-1298. DOI: 10.2147/IJN.S57122

6. Gilmanshina TR, Mamina LI, Koroleva GA, Bezrukikh AI. On the possibility of using oxidized and expanded crystalline graphites in foundry production. *Metallurgiya mashinostroeniya*. 2007;6:22-25. (In Russ.)

7. Kyei-Manu WA, Herd CR, Chowdhury M, Busfield JJC, et al. The influence of colloidal properties of carbon black on static and dynamic mechanical properties of natural rubber. *Polymers*. 2022;14(6):1194. DOI: 10.3390/polym14061194

8. Rutherford KJ, Akutagawa K, Ramier JL, Tunnicliffe LB, et al. The influence of carbon black colloidal properties on the parameters of the Kraus model. *Polymers*. 2023;15(7):1675. DOI:10.3390/polym15071675

9. Maas M. Carbon nanomaterials as antibacterial colloids. *Materials*. 2016;9(8):617. DOI:10.3390/ma9080617

10. Zhang C, Zheng Y, Lin X, Weng S. Research progress on the preparation, performance, mechanisms, and applications of carbon nanomaterials against gram-negative bacteria. *RSC Advances*. 2025;15(28):22180-22201. DOI:10.1039/D5RA01704A

11. Li Q, Noffke BW, Liu Y, Li LS. Understanding fundamental processes in carbon materials with well-defined colloidal graphene quantum dots. *Current Opinion in Colloid & Interface Science*. 2015;20(5-6):346-353. DOI:10.1016/j.cocis.2015.10.008

12. Shafi Z, Pandey VK, Singh R, Rustagi S. Carbon dots-nanosensors: advancement in food traceability for a sustainable environmental development. *Food Control*. 2024;165:110693. DOI:10.1016/j.foodcont.2024.110693

13. Damasceno JPV, Marques FB. Aqueous dispersion of *n*-doped graphite and the electronic stabilization of lyophobic colloids. *Journal of Colloid and Interface Science*. 2025;698:138074. DOI:10.1016/j.jcis.2025.138074

14. Draude AP, Dierking I. Lyotropic liquid crystals from colloidal suspensions of graphene oxide. *Crystals*. 2019;9(9):455. DOI:10.3390/cryst9090455

15. Keinänen P, Siljander S, Koivula M, Sethi J, et al. Optimized dispersion quality of aqueous carbon nanotube colloids as a function of sonochemical yield and surfactant/CNT ratio. *Heliyon*. 2018;4(9):e00787. DOI: 10.1016/j.heliyon.2018.e00787

16. Pavía M, Emo M, Estellé P, Rahman Mohamed A, et al. Controlled structural damaging of multiwalled carbon nanotubes and graphene nanoplatelets by oxidation for stable nanofluids with enhanced thermal conductivity. *Journal of Molecular Liquids*. 2023;390:123194. DOI: 10.1016/j.molliq.2023.123194

17. Gubernat M, Tomala J, Frohs W, Fraczek-Szczypta A, et al. De-agglomeration and homogenisation of nanoparticles in coal tar pitch-based carbon materials. *Journal of Nanoparticle Research*. 2016;18(3):1-13. DOI: 10.1007/s11051-016-3362-9

18. Nemanich RJ, Solin SA. First- and second-order Raman scattering from finite-size crystals of graphite. *Physical Review B*. 1979;20(2):392–401. DOI:10.1103/PhysRevB.20.392

19. Cançado LG, Takai K, Enoki T, Endo M, et al. Measuring the degree of stacking order in graphite by Raman spectroscopy. *Carbon.* 2008;46(2):272-275. DOI: 10.1016/j.carbon.2007.11.015

20. Ferrari AC, Meyer JC, Scardaci V, Casiraghi C, et al. Raman spectrum of graphene and graphene layers. *Physical Review Letters*. 2006;97(18):187401. DOI:10.1103/PhysRevLett.97.187401

21. Wu JB, Lin ML, Cong X, Liu HN, et al. Raman spectroscopy of graphene-based materials and its applications in related devices. *Chemical Society Reviews*. 2018;47(5):1822-1873. DOI:10.1039/C6CS00915H

22. Goncharova N, Samoilov V, Elchaninova V, Nakhodnova A, et al. Estimation of graphene layers number and defectiveness of few-layered graphene particles by Raman spectroscopy. *Journal of Advanced Materials and Technologies*. 2024;9(2):84-90. DOI: 10.17277/jamt.2024.02.pp.084-090

23. Sosedov VP. (ed.) *Properties of Carbon-Based Structural Materials*. Moscow: Metallurgiya; 1975. 335 p. (In Russ.)

24. Ostrovsky VS. *Fundamentals of Artificial Graphite Materials Science.* Moscow: Metallurg izdat; 2011. 111 p. (In Russ.)

25. Park S, An J, Piner RD, Jung I, et al. Aqueous suspension and characterization of chemically modified graphene sheets. *Chemistry of Materials*. 2008;20(21): 6592-6594. DOI:10.1021/cm801932u

26. Radoń A, Włodarczyk P, Łukowiec D. Structure, temperature and frequency dependent electrical conductivity of oxidized and reduced electrochemically exfoliated graphite. *Physica E: Low-dimensional Systems and Nanostructures*. 2018;99:82-90. DOI:10.1016/j.physe.2018.01.025

27. Woznica N, Hawelek L, Fischer HE, Bobrinetskiy I, et al. The atomic scale structure of graphene powder studied by neutron and X-ray diffraction. *Journal of Applied Crystallography*. 2015;48(5):1429-1436. DOI: 10.1107/S1600576715014053

28. Bukalov SS, Zubavichus YV, Leites LA, Sorokin AI, et al. Structural changes in industrial glassy carbon as a function of heat treatment temperature according to Raman spectroscopy and X-ray diffraction data. *Nanosystems: physics, chemistry, mathematics*. 2014;5(1):186-191.

29. Jurkiewicz K, Pawlyta M, Burian A. Structure of carbon materials explored by local transmission electron microscopy and global powder diffraction probes. *C*. 2018;4(4):68. DOI:10.3390/c4040068

30. Le KC, Lefumeux C, Pino T. Differential Raman backscattering cross sections of black carbon nanoparticles. *Scientific Reports*. 2017;7(1):17124. DOI: 10.1038/s41598-017-17300-6

31. Pawlyta M, Rouzaud JN, Duber S. Raman microspectroscopy characterization of carbon blacks: spectral analysis and structural information. *Carbon*. 2015;84:479-490. DOI:10.1016/j.carbon.2014.12.030

32. Salver-Disma F, Tarascon JM, Clinard C, Rouzaud JN. Transmission electron microscopy studies on carbon materials prepared by mechanical milling. *Carbon*. 1999;37(12):1941-1959. DOI:10.1016/S0008-6223(99) 00059-7

33. Samoilov VM, Streletsky AN. Influence of ultra-fine grinding on the crystal structure and graphitability of carbon fillers. *Himiya tverdogo topliva = Solid fuel chemistry*. 2004;2:53-59. (In Russ.)

34. Nikolaeva AV, Samoilov VM, Danilov EA, Mayakova DV, et al. Effectiveness of using surfactants and organic additives in obtaining aqueous suspensions of graphene from natural graphite under the influence of ultrasound. *Perspektivnye materialy = Inorganic Materials: Applied Research*. 2015;2:44-56. (In Russ.)

35. Samoilov VM, Nikolaeva AV, Danilov EA, Erpuleva GA, et al. Preparation of aqueous graphene suspensions by ultrasonication in the presence of a fluorine-containing surfactant. *Inorganic Materials*. 2015;51(2):98-105. DOI:10.1134/S0020168515010161

36. Zhang Z, Schniepp HC, Adamson DH. Characterization of graphene oxide: variations in reported approaches. *Carbon*. 2019;154:510-521. DOI:10.1016/ j.carbon.2019.07.103

37. Nemanich RJ, Lucovsky G, Solin SA. Infrared active optical vibrations of graphite. *Solid State Communications*. 1977;23(2):117-120. DOI:10.1016/0038-1098(77)90663-9

38. Lai SK, Tong LH, Lim CW. On the reflection and diffraction of carbon nanotube array thin film. *Wave Motion*. 2019;90:196204. DOI:10.1016/j.wavemoti.2019. 04.005

39. Cui K, Wardle BL. Breakdown of native oxide enables multifunctional, free-form carbon nanotube–metal hierarchical architectures. *ACS Applied Materials & Interfaces*. 2019;11(38):35212-35220. DOI:10.1021/acsami. 9b08290

40. Damnjanović M, Vuković T, Milošević I. Diffraction from carbon nanotubes. *Materials Science and Engineering: B*. 2011;176(6):497-499. DOI:10.1016/ j.mseb.2010.05.006

41. Ban S, Malek K, Huang C, Liu Z. A molecular model for carbon black primary particles with internal nanoporosity. *Carbon*. 2011;49(10):3362-3370. DOI:10.1016/ j.carbon.2011.04.044

42. Nasibi M, Golozar MA, Rashed G. Nanoporous carbon black particles as an electrode material for electrochemical double layer capacitors. *Materials Letters*. 2013;91:323-325. DOI:10.1016/j.matlet.2012.09.088

43. Zhang W, Yin B, Akbar A, Li WW, et al. Nano-micro pore structure characteristics of carbon black and recycled carbon fiber reinforced alkali-activated materials. *npj Materials Sustainability*. 2024;2(1):30. DOI:10.1038/ s44296-024-00033-9

44. Borah D, Satokawa S, Kato S, Kojima T. Characterization of chemically modified carbon black for sorption application. *Applied Surface Science*. 2008; 254(10):3049-3056. DOI:10.1016/j.apsusc.2007.10.053

45. Danilov EA, Samoilov VM, Dmitrieva VS, Nikolaeva AV, et al. Manufacturing transparent conducting films based on directly exfoliated graphene particles via Langmuir–Blodgett technique. *Inorganic Materials: Applied Research*. 2018;9(5):794-802. DOI: 10.1134/S2075113318050064

46. Cai W, Zhu Y, Li X, Piner RD, et al. Large area few-layer graphene/graphite films as transparent thin conducting electrodes. *Applied Physics Letters*. 2009;95(12):123115. DOI:10.1063/1.3220807

47. Pantea D, Darmstadt H, Kaliaguine S, Sümmchen L, et al. Electrical conductivity of thermal carbon blacks. *Carbon*. 2001;39(8):1147-1158. DOI:10.1016/S0008-6223 (00)00239-6

48. Khodabakhshi S, Fulvio PF, Andreoli E. Carbon black reborn: structure and chemistry for renewable energy harnessing. *Carbon*. 2020;162:604-649. DOI:10.1016/ j.carbon.2020.02.058

Information about the authors / Информация об авторах

Natalia N. Goncharova, Head of the Project, Private institution for the scientific development of the nuclear industry "Science and innovation", Moscow, Russian Federation; ORCID 0009-0003-6722-1246; e-mail: NatNGoncharova@rosatom.ru

Гончарова Наталья Николаевна, руководитель направления, Частное учреждение «Наука и инновации», Москва, Российская Федерация; ORCID 0009-0003-6722-1246; e-mail: NatNGoncharova@rosatom.ru

Vladimir M. Samoilov, D. Sc. (Eng.), Chief Researcher, JSC Scientific Research Institute of Structural Materials Based on Graphite "NIIgrafit" (JSC "NIIgrafit"), Moscow, Russian Federation; ORCID 0000-0002-9861-905X; e-mail: VMSamoylov@rosatom.ru

Самойлов Владимир Маркович, доктор технических наук, главный научный сотрудник, АО «Научно-исследовательский институт конструкционных материалов на основе графита «НИИграфит» (АО «НИИграфит»), Москва, Российская Федерация; ORCID 0000-0002-9861-905X; e-mail: VMSamoylov@rosatom.ru

Egor A. Danilov, Cand. Sc. (Chem.), Head of Functional Materials Department, JSC "NIIgrafit", Moscow, Russian Federation; ORCID 0000-0002-1986-3936; e-mail: egadanilov@rosatom.ru

Данилов Егор Андреевич, кандидат химических наук, начальник управления функциональных материалов, АО «НИИграфит», Москва, Российская Федерация; ORCID 0000-0002-1986-3936; e-mail: egadanilov@rosatom.ru

Anastasiya V. Nakhodnova, Cand. Sc. (Eng.), Head of the Testing Center, JSC "NIIgrafit", Moscow, Russian Federation; ORCID 0000-0002-7862-6789; e-mail: AVNakhodnova@rosatom.ru

Находнова Анастасия Васильевна, кандидат технических наук, начальник испытательного центра, АО «НИИграфит», Москва, Российская Федерация; ORCID 0000-0002-7862-6789; e-mail: AVNakhodnova@rosatom.ru

Boris S. Kleusov, Senior Researcher, JSC "NIIgrafit", Moscow, Russian Federation; ORCID 0000-0003-3924-2616; e-mail: BSKleusov@rosatom.ru

Клеусов Борис Сергеевич, старший научный сотрудник, АО «НИИграфит», Москва, Российская Федерация; ORCID 0000-0003-3924-2616; e-mail: BSKleusov@rosatom.ru

Maksim V. Gudkov, Cand. Sc. (Chem.), Senior Researcher, N. N. Semenov Federal Research Center for Chemical Physics Russian Academy of Sciences, Moscow, Russian Federation; ORCID 0000-0002-9049-9495; e-mail: gudkovmv@chph.ras.ru

Гудков Максим Владимирович, кандидат химических наук, старший научный сотрудник, Федеральный исследовательский центр химической физики им. Н. Н. Семенова РАН, Москва, Российская Федерация; ORCID 0000-0002-9049-9495;e-mail: gudkovmv@chph.ras.ru

Nikolai I. Novosadov, Junior Researcher, N. N. Semenov Federal Research Center for Chemical Physics Russian Academy of Sciences, Moscow, Russian Federation; ORCID 0009-0004-1707-2286; e-mail: novosadovni@chph.ras.ru

Новосадов Николай Иванович, младший научный сотрудник, Федеральный исследовательский центр химической физики им. Н. Н. Семенова РАН, Москва, Российская Федерация; ORCID 0009-0004-1707-2286, e-mail: novosadovni@chph.ras.ru

Vlada A. Goncharova, Intern Researcher, JSC "NIIgrafit", Moscow, Russian Federation; ORCID 0009-0003-6955-5784; e-mail: vlagoncharova@rosatom.ru

Гончарова Влада Андреевна, стажер-исследователь, АО «НИИграфит», Москва, Российская Федерация; ORCID 0009-0003-6955-5784; e-mail: vlagoncharova@rosatom.ru

Received 15 January 2026; Revised 27 February 2026; Accepted 05 March 2026